Multilayer Dual-Mode Dual-Band Filter Using Square Loop Resonators

Vasa Radonić, Vesna Crnojević-Bengin

Faculty of Technical Sciences, University of Novi Sad
Trg Dositeja Obradovića 6, Novi Sad, Serbia
vasarad@uns.as.rs
bengin@uns.ac.rs

***Abstract*— In this paper, a multilayer dual-band dual-mode band pass filter based on square loop resonators is proposed, which allows independent tuning of both resonant frequencies and both pass band bandwidths. The filter is realized on two stacked Taconic CεR-10 substrates, where one resonator is positioned in the upper layer and other one in the middle layer between feed lines and the ground. Despite a similarity of resonators, the coupling and feeds locations in regards to resonators in the filter, they operate at different bands. The influence of different geometrical parameters on the filter performances is analyzed: size of perturbation elements, loops length, loops width and substrate thickness. The fabricated filter has two pass bands positioned at 2.49GHz and 3.55GHz with 3dB bandwidths equal to 80.3MHz and 69.8MHz, respectively. Currently, optimization is underway to precisely comply with IEEE WLAN 802.11 b/g and the IEEE WiMAX 802.16 standard frequencies (i.e. at 2.4GHz and 3.5GHz).**

I. Introduction

Since the dual-mode characteristic of the ring resonator was analyzed by Wolff and Knoppik in 1971, [1] dual-mode resonators has received significant attention. Dual-mode resonators are attractive because each dual-mode resonator can be used as a doubly tuned resonant circuit and, therefore, number of resonators required for a given filter degree is reduced by half, resulting in a compact filter configuration. For a dual-mode operation, a perturbation has to be introduced in a resonator in order to couple its two degenerate modes. Their dual-mode nature give them good performances including small size, low radiation losses, high Q values and easy tuning with great filtering capabilities.

As the number of different wireless systems and services is rapidly growing, frequencies become less available. A solution to this problem is multi-band operation of modern wireless communication systems, on arbitrary frequencies. Therefore, the band pass filters are necessitated that operate at two or more non-harmonically related frequency bands.

In the recent years, there have been significant developments in the field of dual-mode resonators. One idea is to design high performance and selective dual-mode filter with adjustable second pass band for dual-band operation, [2]. Another idea is based on coupling two dual-mode resonators to obtain dual-band behavior, [3]-[5]. Recently, different band pass dual-mode dual-band filters have been proposed, such as a filter based on double square-loop structure with easily tunable higher pass band, [3], a filter based on two loops that uses loading elements to excite dual-mode behavior, [4] as well as a very compact high selective filter based on double-triangular configuration with low insertion losses, [5].

In this paper, novel configuration of multilayer dual-band dual-mode filter is proposed. The filter is realized on two-layer substrate with strong capacitive coupling between the loops. Geometrical arrangement of loops causes positive coupling effect that results in low losses in the pass bands. Superposition method is used to determine how each element affects filter performances. In order to optimize the pass bands characteristics, the influence of different geometrical parameters on the dual-mode dual-band filter performances is analyzed in detail, namely size of perturbation elements, loops length and width, and substrates thicknesses. The proposed dual-mode dual-band filter is fabricated using standard PCB technology on the Taconic CεR-10 substrate. It exhibits two independently controlled pass bands positioned at 2.49GHz and 3.55GHz with 3dB bandwidths equal to 80.3MHz and 69.8MHz and measured insertion losses of -2.6dB and -3.47dB, respectively.

II. Dual-Band Dual-Mode Filter Design

The proposed dual-band dual-mode band pass filter consists of two capacitively coupled square loop resonators positioned in adjacent conductive layers. Layouts of both conductive layers are shown in Fig. 1, while Fig. 2 shows 3-D view of the circuit. T-shaped feed lines are used in both layers to increase the coupling between the feed lines and the resonators. The connection between adjacent conductive layers is realized by vias, modeled with square 0.4mm x 0.4mm cross section. Due to such configuration, the lower resonator is fed from the outside while the upper resonator is fed from the inside. Square perturbation elements are introduced in the resonators at a location that is offset 135 degrees from the feeds. To avoid interference between resonators, their perturbations are positioned on the opposite sides of loops.

The value g denotes the gap between the loops and the T-shaped feed lines, while a_1 and a_2 denote the size of the square perturbation elements. Widths of the feed lines, their T-shaped segments and both loops are denoted by w_i, w, and w_1 and w_2, respectively, while l_1 and l_2 are side-lengths of the two loops.

The filter is realized on substrate that consists of two layers, with thicknesses h_1 = 1.27mm and h_2 = 0.64mm. Taconic CεR-10 substrate with ε_r = 9.8 and dielectric loss tangent equal to 0.0035 is used in both layers. To enhance the coupling between feeds and the resonators, the gap g is chosen to be the minimal available in standard PCB technology, i.e. equal to 100µm. Conductor losses are modeled using bulk conductivity for copper. The initial dimensions of proposed dual-mode dual-band filter are: l_1 = 13.5mm, l_2 = 9mm, w_i = 1.1mm, w = 1mm, w_1 = 1.5mm, w_2 = 1.9mm, a_1 = 1mm and a_2 = 0.5mm.

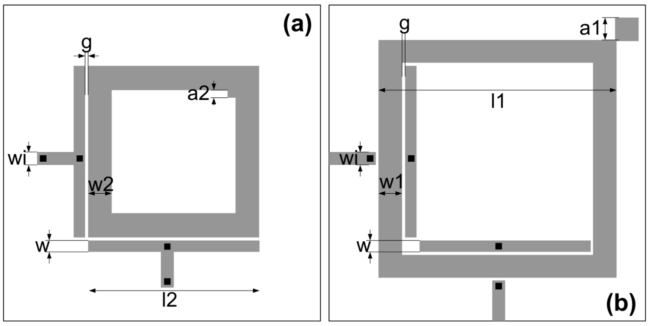

Fig. 1. Layout of the filter: (a) middle conductive layer (layer2), (b) top conductive layer (layer1)

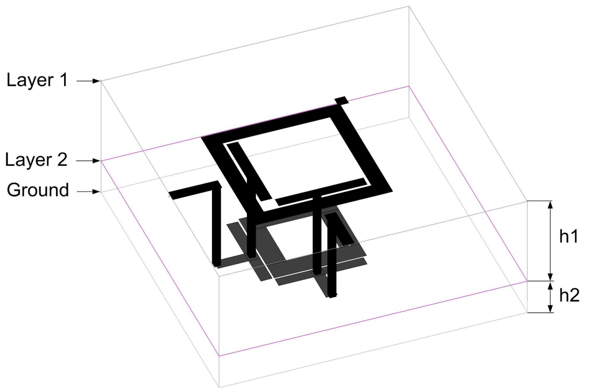

Fig. 2. 3-D view of the proposed dual-band dual-mode filter (for clarity, ground is not shown in separate color).

To understand its electromagnetic behavior, the dual-mode dual-band filter is analyzed using superposition method, i.e. it is divided into two single dual-mode configurations. Simulation results for the two resonators are shown in Fig. 3, together with the response of the proposed dual-band dual-mode filter. Simulations were performed using EMSight, EM simulator in Microwave Office. Numerical results are summarized for all analyzed cases in Table I, where f_{r1} represents resonant frequency of the first pass band which originates from the Layer1 resonator, while f_{r2} represents resonant frequency of the second pass band which originates from the Layer2 resonator. BW_1 and BW_2 are 3dB bandwidths of the two resonators, and s_{21}^1 and s_{21}^2 are insertion losses in the first and the second pass band, respectively.

Fig. 3 and Table I reveal that resonant frequencies of each dual-mode resonators almost coincide with those of the dual-band dual-mode filter. Also, it can be noted that coupling between two resonators influences the positions of transmission zeros and decrease attenuation in comparison to individual resonators.

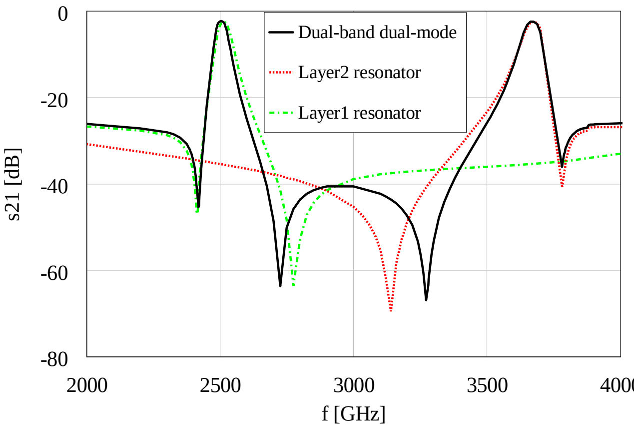

Fig. 3. Simulation results for two dual-mode resonators and the proposed dual-band dual-mode filter.

TABLE I. NUMERICAL RESULTS FOR TWO DUAL-MODE RESONATORS AND PROPOSED DUAL-BAND DUAL-MODE FILTER.

	Layer1 resonator	**Layer2 resonator**	**Proposed filter**
f_1 [GHz]	2.514	na	2.505
f_2 [GHz]	na	3.675	3.668
BW_1 [MHz]	47.9	na	44.5
BW_2 [MHz]	na	65.2	66.1
s_{21}^1 [dB]	2.444	na	2.304
s_{21}^2 [dB]	na	2.44	2.41

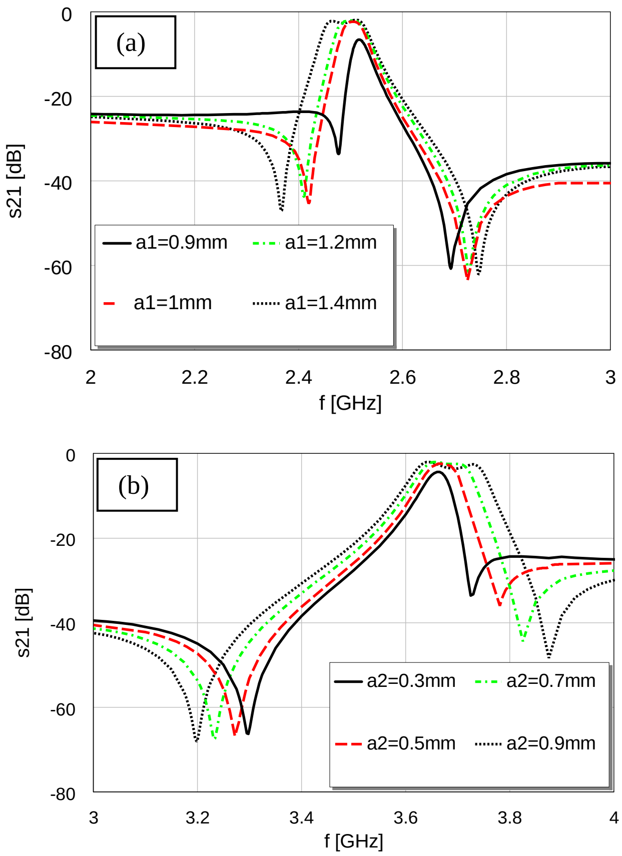

Fig. 4. Influence of the perturbations size to dual-band dual-mode characteristic: (a) influence of a_1 for a_2 fixed, (b) influence of a_2 for a_1 fixed

In order to investigate how the dimensions of perturbation affect characteristics, the perturbation sizes are varied. Simulation results for four different values of a_1 and a_2 are shown in Fig. 4a and Fig. 4b, respectively. The figure shows particular part of the graphic, which passband is influenced by changing of parameter. When a_1 changes, parameter a_2 has constant value equal to 0.5mm. Likewise, when a_2 changes, parameter a_1 has constant value equal to 1mm.

Fig. 4 reveals that change of the perturbation size has small effect on the resonant frequency, but affects the shape of the pass band and its selectivity. As the perturbation size increases, the insertion losses are decreased and, at the same time, the bandwidth is increased while the positions of transmission zeros are changed. Furthermore, it can be noted that a_1 influences only the first pass band, while a_2 influences only the second one. For example, by reducing the perturbation a_2 from 0.7 mm to 0.3 mm, increase of the second bandwidth for more then 118% can be obtained. At the same time, the insertion losses in the second pass band are decreased for 2dB.

To determine how the loop line widths influence the response of the proposed filter, configurations with four different values of w_1 and w_2 have been analyzed. Simulation results are shown in Fig. 5. When parameter w_1 changes, w_2 has constant value equal to 1.9mm. Likewise, when w_2 changes, parameter w_1 has constant value equal to 1.5mm.

The first resonance is decreased when w_1 is increased, while the second resonance increases with w_2. Change of the loop line width has strong influence only on the position of the corresponding pass band and transmission zeros, while its effect on the insertion loss and the bandwidth is negligible.

The influence of lengths of both loops, l_1 and l_2, have also been analyzed and the simulation results are shown in Fig. 6. When l_1 changes, parameter l_2 has constant value equal to 9mm. Likewise, when l_2 changes, parameter l_1 has constant value equal to 13.5mm.

It can be seen that the resonant frequency is shifted towards lower frequencies as the ring length is increased, due to increasing inductance of the loops. Change of the ring has strong influence on the positions of the correspondent passband and transmission zeros. By increasing the lengths, the corresponding bandwidth is also increased. This effect is stronger in the case of upper resonator.

The proposed filter is designed on two layers of substrate with the same dielectric properties. The layers' thicknesses strongly influence the coupling between two dual-mode resonators. This is analyzed in Fig. 7.

The thicknesses of the layers influence the position of the pass bands and transmission zeros as well as the insertion losses in the pass bands. In addition, by changing the thicknesses, the attenuation in the stop band can be increased. Additional optimization of perturbations size and loop line widths will enable obtaining different specifications of bandwidths.

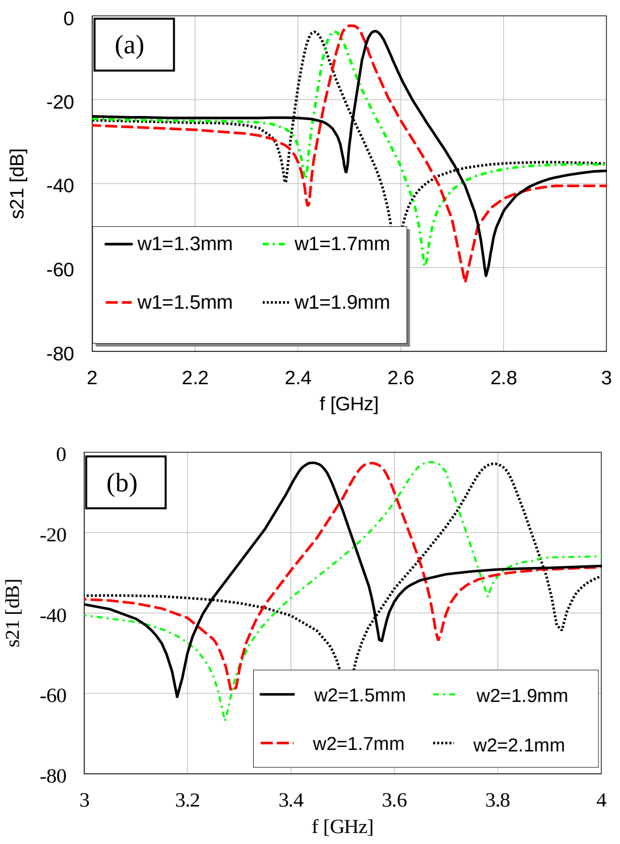

Fig. 5. Influence of the loop line width to dual-mode dual-band filter characteristic: (a) influence of w_1 for w_2 fixed, (b) influence of w_2 for w_1 fixed

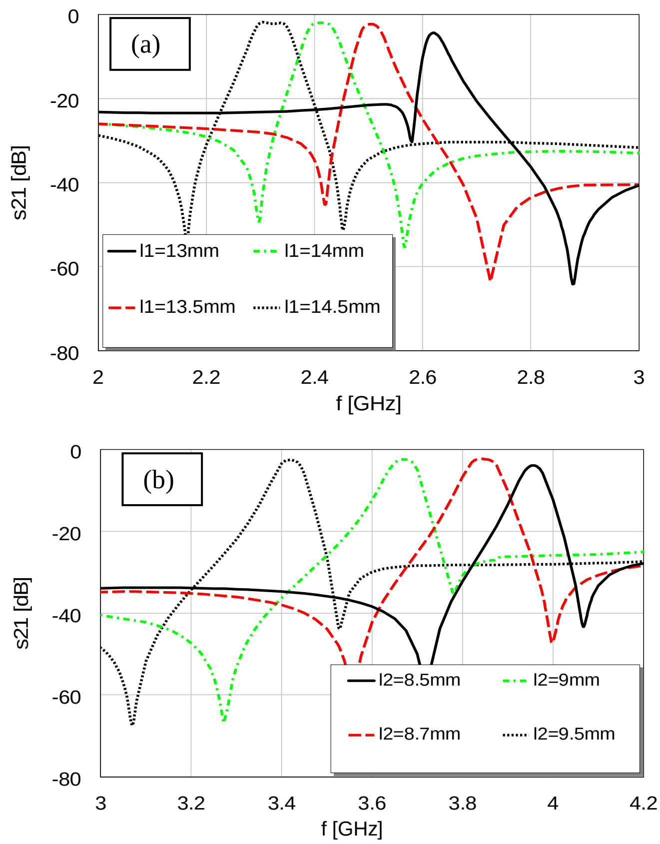

Fig. 6. Influence of the loop size to filter characteristic: (a) influence of l_1 for l_2 fixed, (b) influence of l_2 for l_1 fixed

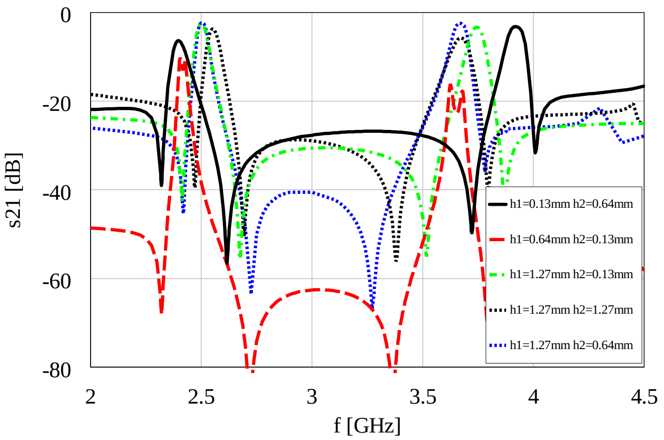

Fig. 7. Influence of the substrate thicknesses to the dual-band dual-mode filter characteristic.

III. FABRICATION

The proposed filter was fabricated in standard PCB technology on two Taconic CεR-10 substrates with thicknesses 1.27 mm for the upper layer and 0.64 mm for the bottom layer. Photographs of upper sides of both layers are shown in Fig. 8. Two layers are stacked after being separately etched, using Bison epoxy glue. The overall dimensions of the filter are equal to 15.9mm x 15.9mm, i.e. $0.35\lambda_g$ x $0.35\lambda_g$, where λ_g denotes the guided wavelength.

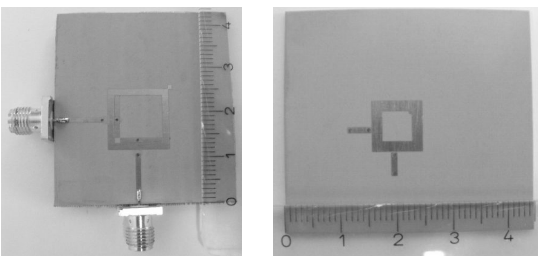

Figure 8. Photograph of the fabricated dual-band dual-mode filter.

Simulated and measured results are compared in Fig. 9. Measured central frequencies of the pass bands are 2.49GHz and 3.55GHz, insertion losses are equal to -2.6dB and -3.47dB, and 3dB bandwidths are 80.3MHz and 69.8MHz, respectively. The central frequency of the second pass band is significantly shifted towards lower frequencies. This is the direct consequence of imperfect multi-layer fabrication process: the thickness of the epoxy glue and its electrical characteristics influence the filter performances, particularly the resonance of the loop in Layer 2. This has also been verified trough additional simulations where the epoxy layer has been modeled. A new prototype is being fabricated using an improved procedure, with dimensions optimized to operate according to IEEE WLAN 802.11 b/g and the IEEE WiMAX 802.16 standards.

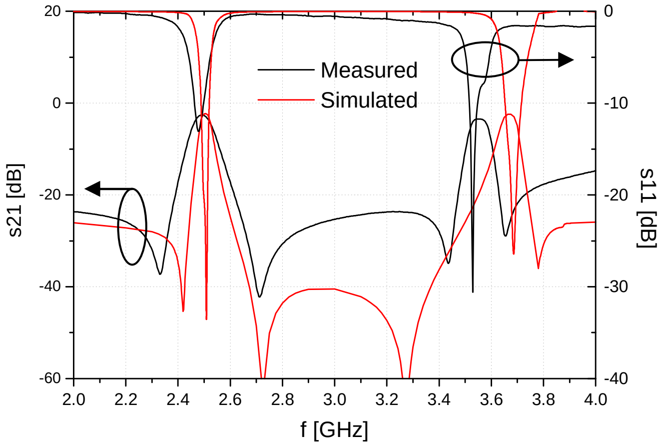

Fig. 9. Measured and simulated responses of the proposed filter

IV. CONCLUSIONS

In this paper, multilayer dual-band dual-mode band pass filter is proposed, based on two capacitively coupled square loop resonators. By using superposition method, dual-mode resonators are separately designed so the filter exhibits two pass bands whose positions and bandwidths can be individually tuned. The influence of different geometrical parameters on the filter performances has been analyzed in detail. A prototype has been fabricated using standard PCB technology. Small attenuation in the pass bands, compact design and easy way to tune, make this dual-mode dual-band filter suitable for many wireless applications.

REFERENCES

[1] Wolff. I. and Knoppik. N. (1971). Microstrip Resonator and Dispersion Measurements on Microstrip Lines. *Electronics Lett.* vol. 7, Issue 26, pp. 779–781, December 1971

[2] T.-H. Huang, H.-J. Chen, C.-S. Chang, L.-S. Chen, Y.-H. Wang, and M.-P. Houng, “A novel compact ring dual-mode filter with adjustable second passband for dual-band applications,“ *IEEE Microwave and Wirelles Components Lett.* vol. 16, no. 6, June 2006.

[3] H. Chen, X.-W. Dai, and C.-H. Liang, “Novel dual-mode dual-band bandpass filter using double square-loop structure,“ *Progress In Electromagnetic Research*, PIER 77, pp. 409-416, 2007

[4] c. Karpuz, and A. Gorur, “Dual-mode dual-band microstrip filters.” *Proceeding of the 39th European Microwave Conference*, Rome, 2009

[5] L.-P. Zhao, X.-W. Dai, Z.-X. Chen, and C.-H. Liang, “Novel design of dual-mode dual-band bandpass filter with triangular resonators,” *Progress In Electromagnetic Research*, PIER 77, pp. 417-424, 2007